DFT based computational study on the excited state intramolecular proton transfer processes in o-hydroxybenzaldehyde

ARTICLE *in* SPECTROCHIMICA ACTA PART A MOLECULAR AND BIOMOLECULAR SPECTROSCOPY · AUGUST 2008

Impact Factor: 2.35 · DOI: 10.1016/j.saa.2008.06.032 · Source: PubMed

7 AUTHORS, INCLUDING:

Gobinda Prasad Sahoo
Vidyasagar University
28 PUBLICATIONS **675** CITATIONS
SEE PROFILE

Ajay Misra
Vidyasagar University
56 PUBLICATIONS **903** CITATIONS
SEE PROFILE

Spectrochimica Acta Part A 71 (2009) 1728–1735

Contents lists available at ScienceDirect

Spectrochimica Acta Part A: Molecular and Biomolecular Spectroscopy

journal homepage: www.elsevier.com/locate/saa

DFT based computational study on the excited state intramolecular proton transfer processes in *o*-hydroxybenzaldehyde

Sankar Prasad De, Sankarlal Ash, Dipak kumar Bhui, Harekrishna Bar, Priyanka Sarkar, Gobinda Prasad Sahoo, Ajay Misra*

Department of Chemistry and Chemical Technology, Vidyasagar University, Midnapore 721102, West Bengal, India

ARTICLE INFO

Article history:
Received 15 March 2008
Received in revised form 21 May 2008
Accepted 24 June 2008

Keywords:
Excited state intramolecular proton transfer
Intramolecular hydrogen bond
DFT
B3LYP
PE

ABSTRACT

Potential energy (PE) curves for the intramolecular proton transfer in the ground (GSIPT) and excited (ESIPT) states of *o*-hydroxybenzaldehyde (OHBA) were studied using DFT-B3LYP/6-31G(d) and TD-DFT-B3LYP/6-31G(d) level of theory, respectively. Our calculations suggest the non-viability of ground state intramolecular proton transfer in this compound. Excited states PE calculations support the ESIPT process in OHBA. The contour PE diagram and the variation of oscillator strength along the proton transfer co-ordinate support the dual emission in OHBA. Our calculations also support the experimental observations of Nagaoka et al. [S. Nagaoka, U. Nagashima, N. Ohta, M. Fujita, T. Takemura, J. Phys. Chem. 92 (1988) 166], i.e. normal emission of the title compound comes from S_2 state and the red-shifted proton transfer band appears from the S_1' state. ESIPT process has also been explained in terms of HOMO and LUMO electron density of the enol and keto tautomer of OHBA and from the potential energy surfaces.

1. Introduction

Excited state intramolecular proton transfer (ESIPT) reactions are of great scientific and technological interest. Since its introduction, the photoinduced excited state intramolecular proton (or hydrogen) transfer reaction which generally incorporate transfer of a hydroxyl (or amino) proton to the carbonyl oxygen (imine nitrogen) through a pre-existing intramolecular hydrogen bonding (IMHB) configuration, have received considerable attention, because it has led to a wide range of application, such as laser dyes [1,2], polymer stabilizer [3], Raman filters [4], environmental probes in bio-molecules [5], etc. Main requirement of ESIPT reaction is that the molecule must have acid and basic groups and the strong intramolecular hydrogen bond between the two groups at the same time. A large number of molecules belonging to this class, e.g. *o*-hydroxybenzoyl [6–16], *o*-hydroxy Schiff bases [17–20] and so on.

Weller [21,22], in his pioneering work, had pointed out the dual emission in the fluorescence spectra of salicylic acid and methyl salicylate and attributed it to asymmetric double well potential arising from proton transfer in the ground state and also in the excited states as shown in Scheme 1. The two wells in the ground state potential energy curve represents the primary (N) and tautomeric (T) forms, and the two wells in the excited state curve represents the corresponding excited states N* and T*, respectively. It is clear from Scheme 1 that the N form is the most stable in the ground state and T* in the excited state.

Since the original work of Weller [21] on the ESIPT of methyl salicylate (MS), a large number of experimental [23–30] and theoretical [31–37] studies on the ESIPT of a variety of systems have been reported. Among them, MS [38–44] and its related compounds, *o*-hydroxy-acetophenone (OHAP) [45–47] and *o*-hydroxybenzaldehyde (OHBA) [48–51] have been well studied as prototypes of molecules showing ESIPT process. OHBA is the simplest and prototypical example of aromatic molecules with an intramolecular hydrogen bond involving a carbonyl group. It shows a large stokes-shifted emission, which is likely to be emitted from the excited state of proton-transferred keto tautomers [45]. In their schematic presentation of potential surface (for OHBA), Nagaoka et al. [50] showed that the $S_1(\pi)$ state of OHBA is somewhat distorted from that of the S_0 state and the potential surface of the $S_2(\pi)$ state is not largely distorted from that of S_0 state. They also showed schematically that the zero point vibrational level of $S_1(\pi)$ state lies towards the keto tautomer form and the emission of OHBA in the visible region occurs from the keto tautomer. A number of theoretical investigations [48–51] had been carried out by different research groups to understand the ESIPT process in OHBA in terms of its electronic structure. But very little study had been done to understand the ground as well as the excited state potential surface of OHBA using density function theoretical approach. The wide

* Corresponding author. Fax: +91 3222 275329.
E-mail address: ajaymsr@yahoo.co.in (A. Misra).

1386-1425/$ – see front matter © 2008 Elsevier B.V. All rights reserved.
doi:10.1016/j.saa.2008.06.032

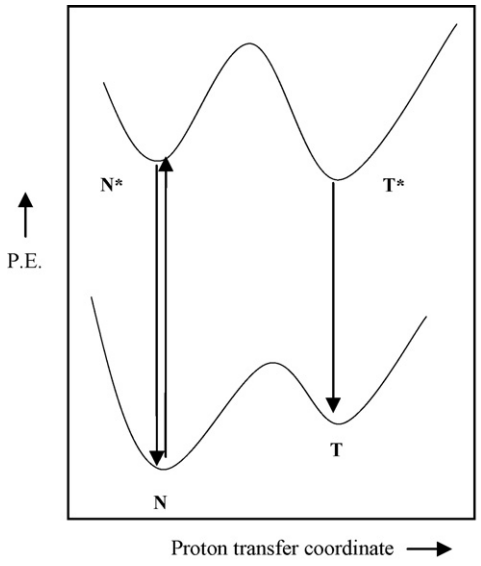

Scheme 1.

spread success of density functional approach for electronic structure calculation [52] and the proposed schematic potential surface of OHBA by Nagaoka et al. [50] motivates us to study the PES of the title compound using DFT approach.

2. Theoretical calculations

Hybrid HF/DFT methods have been proposed as a reliable tools for electronic computation in a general protocol for studying static and dynamic properties of hydrogen-bonded systems [53–55]. One such method, B3LYP [54], proposed and found by Barone and Adamo [55] predicts molecular data that match the available experimental ones. In view of its wide spread success for the calculation of large molecules [56], we decided to choose density functional approach for the present calculation of the excited state proton transfer process in OHBA.

All ab initio calculations reported in this paper were carried out using the Gaussian 03 suite programs [57]. In our previous computational study on the ESIPT process of some naphthalene derivatives [58], and flavones [59], we observed that DFT-B3LYP/6-31G(d) was the best suited with their crystal structure data within our limited computational resource. Keeping our previous success in mind, we decided to use DFT-B3LYP/6-31G(d) method for carrying out present electronic structure calculations on OHBA.

2.1. Methodology for PES calculations

Choice of proton transfer co-ordinate is a challenging task for the ground and excited state potential energy surface calculation. Use of IRC as proton transfer reaction co-ordinate is very much useful for small molecules. In this present problem, conversion from 'N' to 'T' (Scheme 2) in the ground electronic state can be thought of as arising from the transfer of proton from $O_d(2')$ to $O_a(6')$ with simultaneous redistribution of electron density within the six-membered hydrogen bonded ring. Some authors [35] have considered the O_d–O_a distance as fixed and varied the O_d–H bond distance to get an idea about the potential energy curve for both GSIPT and ESIPT processes.

Fig. 1 shows a plot of $O_d(2')$–$O_a(6')$ distance and O_d–H–O_a angle as a function of r_{O_d-H} of OHBA. The plot revels that as the proton shifts from O_d to O_a, the O_d–O_a distance changes significantly. At smaller O_d–H distance (between 0.70 and 0.80 Å) it increases slowly. Then it starts to decrease slowly and in the close vicinity of a stable O_d–H distance, the O_d–O_a distance falls sharply to have a shallow minimum at about 1.30 Å. But on further increase of the

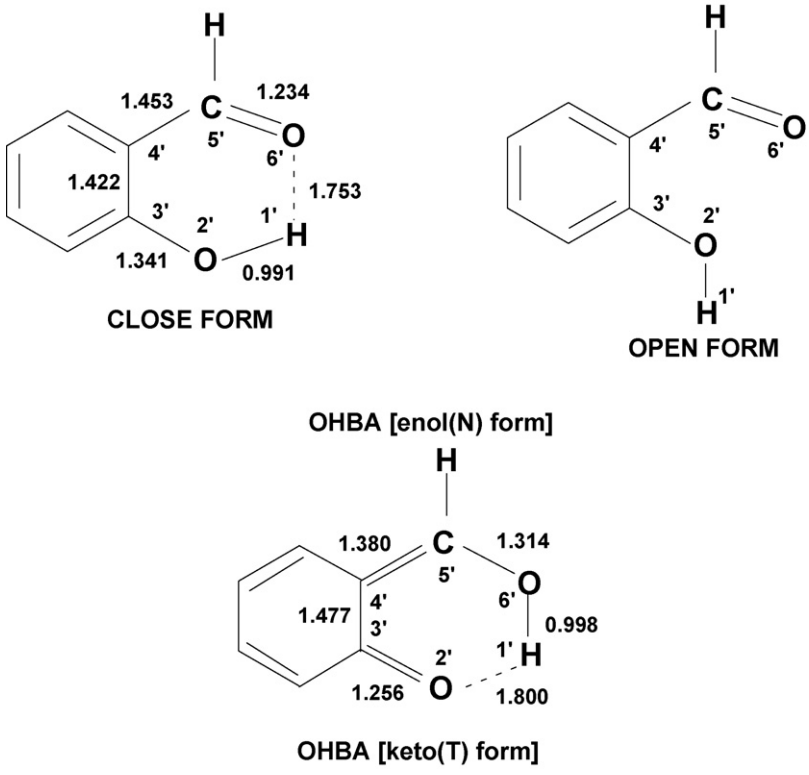

Scheme 2.

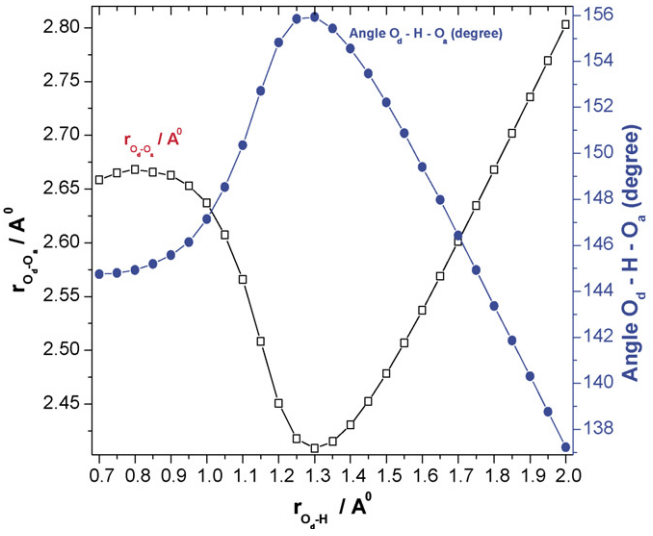

Fig. 1. Variation of $O_d(2')$–$O_a(6')$ distance and O_d–H–O_a angle of OHBA with r_{O_d-H} as obtained from DFT-B3LYP(6-31G(d)) level of theory.

O_d–H distance, it increases sharply and then enlarges to a distance comparable to that in the 'T' form. Again in the Fig. 1, the variation of O_d–H–O_a angle with r_{O_d-H} revels that at smaller O_d–H distance, it increases slowly, then increases sharply in the near vicinity of the stable O_d–H distance (~1.00 Å), reaches maxima and shows a sudden fall with the further increases of r_{O_d-H} distance. Therefore, it is obvious that by freezing the geometry or by fixing the O_d–O_a distance at a particular values, one ends up introducing artificial constraints on the system and hence a barrier for the enol (N) to keto (T) conversion.

On the other hand, choice of $O_d(2')$–H(1′) distance as proton transfer co-ordinate was first proposed by Sobolewski and Domcke [60] and they termed it as 'distinguished co-ordinate approach'. Catalan et al. [53] also used the similar reaction co-ordinate (r_{O-H}) for the ESIPT processes of some naphthalene derivatives. Maheswari et al. [12] did an extensive theoretical study on salicylic acid and showed that the variation of (O_d–H) bond length of hydroxyl group can be used as proton transfer co-ordinate. In recent communications, we reported that the distinguished co-ordinate approach is quite helpful in understanding both the ground and excited state potential energy surface of 1-hydroxy-2-naphthaldehyde, 2-hydroxy-3-naphthaldehyde [58] and 5-hydroxy flavone [59].

In this article we calculated the PES of ground state by varying the $O_d(2')$–H(1′) bond distance from 0.8 to 2.0 Å and rest of the structural parameters are allowed to relax for each choice of $r_{O_d(2')-H(1')}$. Information on the ESIPT curve was obtained by calculating the Franck–Condon (FC) transition energies for the DFT (B3LYP)/6-31G(d) ground state structures at the TD-DFT(B3LYP)/6-31G(d) level. We also calculated the excited state PES using CIS level of theory. A comparison of excited state PES using CIS/6-31G(d) and TD-DFT(B3LYP)/6-31G(d) level of theory as shown in Fig. 2 illustrates that PES using TD-DFT(B3LYP)/6-31G(d) is lower in energy. Again the agreement of TD-DFT(B3LYP)/6-31G(d) result with absorption wavelength (λ_{max}) helps us to use TD-DFT(B3LYP)/6-31G(d) level of theory for excited state PES calculations.

3. Results and discussion

The ground state optimized structure of orthohydroxy benzaldehyde (OHBA) shows that the enol form ('N' form) is the stable form due to the presence of strong intramolecular hydrogen bond (Scheme 2). Bond length, bond angle and dihedral angle data of the six-membered ring system containing intramolecular hydrogen bond of OHBA are shown in Table 1. Ground state bond angle, dihedral angle data of Table 1 suggest that the six-membered ring formed due to intramolecular hydrogen bond in OHBA is planar and it is in the same plane that of the benzene ring.

3.1. Stability due to IMHB

To get an idea about the relative strength of IMHB in OHBA, we compared the C=O and O–H stretching frequencies of this compound with some model compounds like phenol and benzaldehyde (Table 2). The O–H and C=O stretching frequencies were calculated using DFT (B3LYP)/6-31G(d) level of theory. We used 0.9613 as scale factor for frequencies as given in Ref. [60]. Table 2 shows that our methodology works nicely, since our calculated C=O and O–H stretching frequencies agreed well with the experimental results. Hunsberger [61] showed that for the di-substituted compounds (1-hydroxy-2-naphthaldehyde and 2-hydroxy-3-naphthaldehyde), the displacement of the OH band ($\Delta\nu_{OH}$) from its average position in 1-naphthol and 2-naphthol and the displacement of the C=O band ($\Delta\nu_{C=O}$) from its average position in the corresponding mono-substituted, i.e. 2-naphthaldehyde can be taken as a quantitative measure of IMHB strength in the di-substituted compounds. In one of our recent communication [58], we theoretically compared the strength of IMHB between 1-hydroxy-2-naphthaldehyde (1H2NA) and 2-hydroxy-3-naphthaldehyde (2H3NA). Values of $\Delta\nu_{C=O}$ and $\Delta\nu_{OH}$ (Table 2) compare to previously studied compounds 1H2NA ($\Delta\nu_{C=O}$ = 75 and $\Delta\nu_{OH}$ = 511) and 2H3NA ($\Delta\nu_{C=O}$ = 54 and $\Delta\nu_{OH}$ = 329) suggests that the strength of IMHB in OHBA is much weaker.

Vener and Scheiner [35] showed that the associated increase in the extent of the π-system in the 'T' form than that in the 'N' form decreases the gap between the HOMO and LUMO. They also suggested that the extent of decrease of energy gap can be correlated with the strength of the IMHB. This decrease in energy gap between HOMO and LUMO from 'N' to 'T' form is 0.7145 kcal/mol. This small decrease in energy between the HOMO and LUMO on

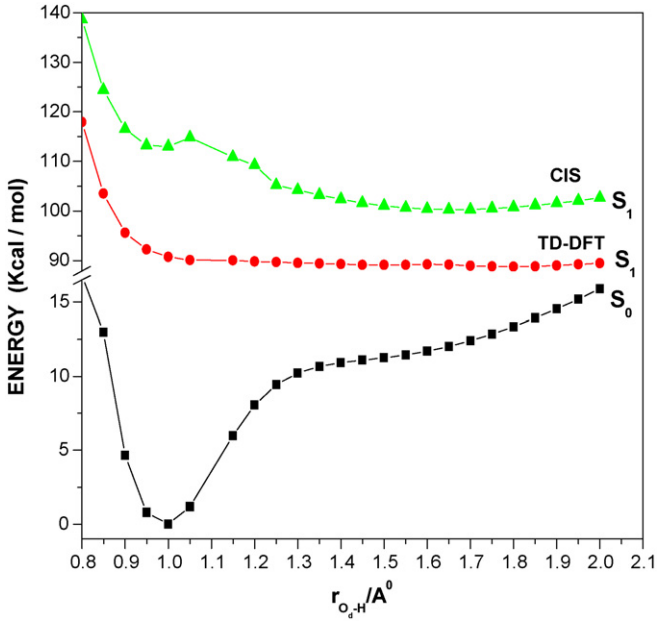

Fig. 2. GSIPT curve (S_0) calculated using 6-31G(d) basis set at B3LYP level for the ground state and ESIPT Franck–Condon curves (S_1) of OHBA indicating the variation of energy (kcal/mol) of OHBA with r_{O_d-H} as obtained from TD-DFT(B3LYP)/6-31G(d) and CIS/6-31G(d) level of theory.

Table 1
Calculated bond length (in Å), bond angle (in degree) and dihedral angle (in degree) at the DFT-B3LYP(6-31G(d)) level for the IMHB ring (Scheme 2) of the 'N' form of OHBA

OHBA		
Bond length	Bond angle	Dihedral angle
H(1′)–O(2′) 0.99123	H(1′)–O(2′)–C(3′) 107.19295	H(1′)–O(2′)–C(3′)–C(4′) 0.00445
O(2′)–C(3′) 1.34087	O(2′)–C(3′)–C(4′) 121.91600	C(3′)–C(4′)–C(5′)–O(6′) 0.00000
C(3′)–C(4′) 1.42169	C(3′)–C(4′)–C(5′) 120.15514	C(5′)–O(6′)–H(1′)–O(2′) 0.03269
C(4′)–C(5′) 1.45314	C(4′)–C(5′)–O(6′) 124.55768	
C(5′)–O(6′) 1.23401	C(5′)–O(6′)–H(1′) 99.23281	
O(6′)–H(1′) 1.75292		

Table 2
Theoretical and experimental carbonyl and hydroxyl stretching frequency values of OHBA, and some model compounds:

Compounds	C=O stretching frequencies (in cm^{-1})		O–H stretching frequencies (in cm^{-1})		$\Delta\nu_{C=O}$		$\Delta\nu_{O-H}$	
	Theo.	Exp.	Theo.	Exp.	Theo.	Exp.	Theo.	Exp.
Phenol			3606	3600				
Benzaldehyde	1731	1700						
OHBA	1670	1666	3219	3061	61	34	387	539

going from 'N' to T tautomeric form of OHBA again suggests that the IMHB strength is weaker in nature.

Relative stability of the enol ('N') form of OHBA was obtained by rotating the phenolic–OH group out of the hydrogen bonded conformation and computing the difference in energy between the closed and open form (Scheme 2). Relative stability due to intramolecular hydrogen bonding for the N tautomer was found to be 12.14 kcal/mol (Fig. 3). This value is comparatively lower in magnitude than our previously studied compounds, i.e. 1H2NA(17.14 kcal/mol), 2H3NA(12.34 kcal/mol)[58] and also 5-hydroxy flavone (14.95 kcal/mol) [59]. Thus the IMHB present in OHBA is comparatively weaker.

3.2. Ground and excited state potential energy curves of OHBA

Potential energy curve of OHBA (Fig. 4) shows that in the ground state of OHBA, enol form ('N') is the most stable tautomeric form. There are no shallow minima of the keto form, rather it is repulsive in nature. Barrier for the enol (N) to keto(T) form is about 12 kcal/mol. This large energy barrier between these two tautomeric forms discarded any possibility of ground state intramolecular proton transfer (GSIPT) under thermal conditions. Again our calculated free energy change for the keto-enol tautomerization of OHBA shows a large +ve value (ΔG = 13.08 kcal/mol). This free energy change gives equilibrium constant for the enol (N) to keto (T) transformation to be 2.52×10^{-10}. These results suggest that N ⇄ T equilibrium lies towards the enol form (N). On the basis of the equilibrium constant, population ratio of enol to keto tautomer in the gas phase is found to be 4.0×10^{9}: 1 and thus confirming the non-viability of the ground state intramolecular proton transfer in OHBA.

GSIPT curve for the keto (T) form is repulsive in nature and the curve in the S_1 state is almost flat with a little downhill while passing from enol to keto form. This downhill nature of the potential energy curve indicates that the excited enol form of OHBA

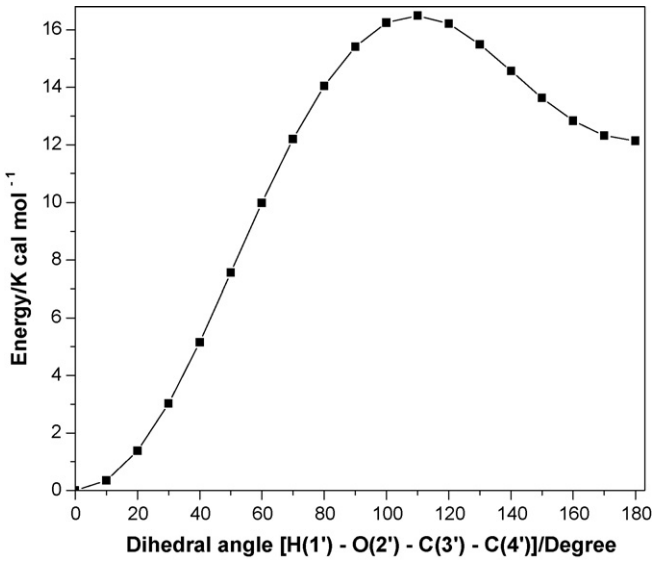

Fig. 3. Energetics of the transformation from IMHB form ('N') to the non-hydrogen bonded form (hydroxyl group rotated by 180°) of OHBA. For each value of dihedral angle (H(1′)–O(2′)–C(3′)–C(4′)), the geometry has been optimized using the DFT-B3LYP(6-31G(d)) level of theory.

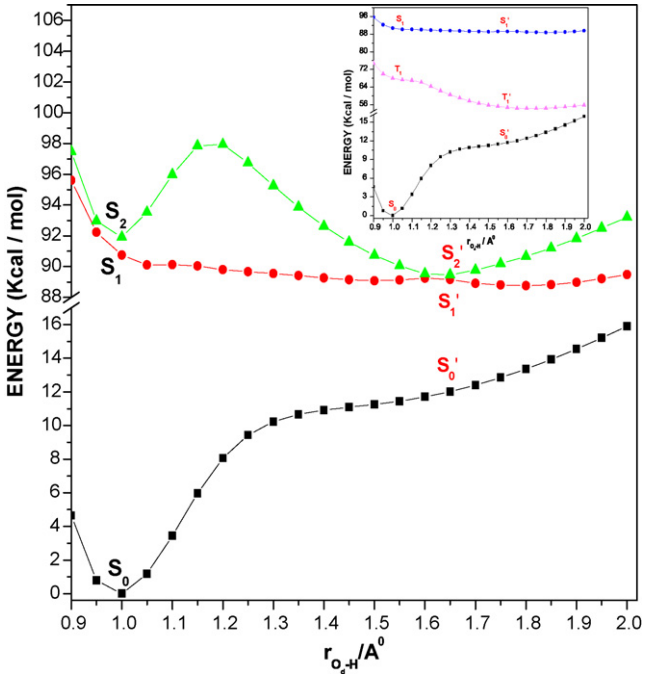

Fig. 4. GSIPT curve (S_0) and ESIPT Franck–Condon curves (S_1 and S_2) of OHBA as obtained from DFT-B3LYP(6-31G(d)) and TD-DFT(B3LYP)/6-31G(d) level of theory. Inset: GSIPT curve (S_0) and ESIPT Franck–Condon curves (S_1 and T_1) of OHBA obtained using the above methodology.

in the S_1 state may pass to the keto form by ESIPT process. This keto form of OHBA shows proton transfer emission. Repulsive nature of the ground state PES of keto tautomer suggests that the proton transfer fluorescence of OHBA will be abroad and structureless. Interestingly, in their experimental work Nagaoka et al. [45] observed broad, structureless emission spectrum of OHBA in 3-methylpentane having $\lambda_{em.} \approx 510$ nm. Nagaoka et al. [49] also observed a red-shifted absorption band of OHBA that is π–π^* in nature with $\lambda_{max} = 320$ nm in ethanol. On the other hand, our gas phase calculation shows $\pi \rightarrow \pi^*$ transition with $\lambda_{max} = 315$ nm for the enol (N) tautomer and this is in good agreement with the experimental findings of Nagaoka et al. [49]. The high potential barrier while passing from N* to T* along the S_2 potential surface discards the possibility of ESIPT in S_2' this state.

3.3. Nature of the ESIPT emission

Fig. 4 shows that the first excited singlet state, i.e. $^1(\pi\pi^*)$ state potential energy curve of OHBA is almost flat, decreasing very slowly with the increase of r_{O_d-H} value after $r_{O_d-H} = 1.0$ Å. Now, if the proton transfer process or any other non-radiative deactivation channel is quite fast compare to the lifetime of excited N-tautomer, as observed by Nagaoka et al. [50] for OHBA, it will be very difficult to observe the emission from N-tautomer. On the other hand, due to the faster formation rate, population of T-tautomer will be high enough to observe emission. Fig. 4 illustrates that the second excited singlet state (S_2) contains two minima, one at $r_{O_d-H} = 1.0$ Å and another at $r_{O_d-H} = 1.55$ Å along the proton transfer coordinate. Minima at $r_{O_d-H} = 1.0$ Å is due to the excited enol form (N*) and at $r_{O_d-H} = 1.55$ Å is of excited keto form (T*). Small energy gap between S_1 and S_2 state of the enol form ($r_{O_d-H} = 1.0$ Å) indicates that both S_1 and S_2 excitation may take place simultaneously. But due to large energy barrier (6 kcal/mol) while passing from enol to keto form in the S_2 state, the excited enol form may decay radiatively to the ground state and this results the normal emission of OHBA. Nagaoka et al. [45] in their experimental work observed the dual emission from excited OHBA. They reported that normal

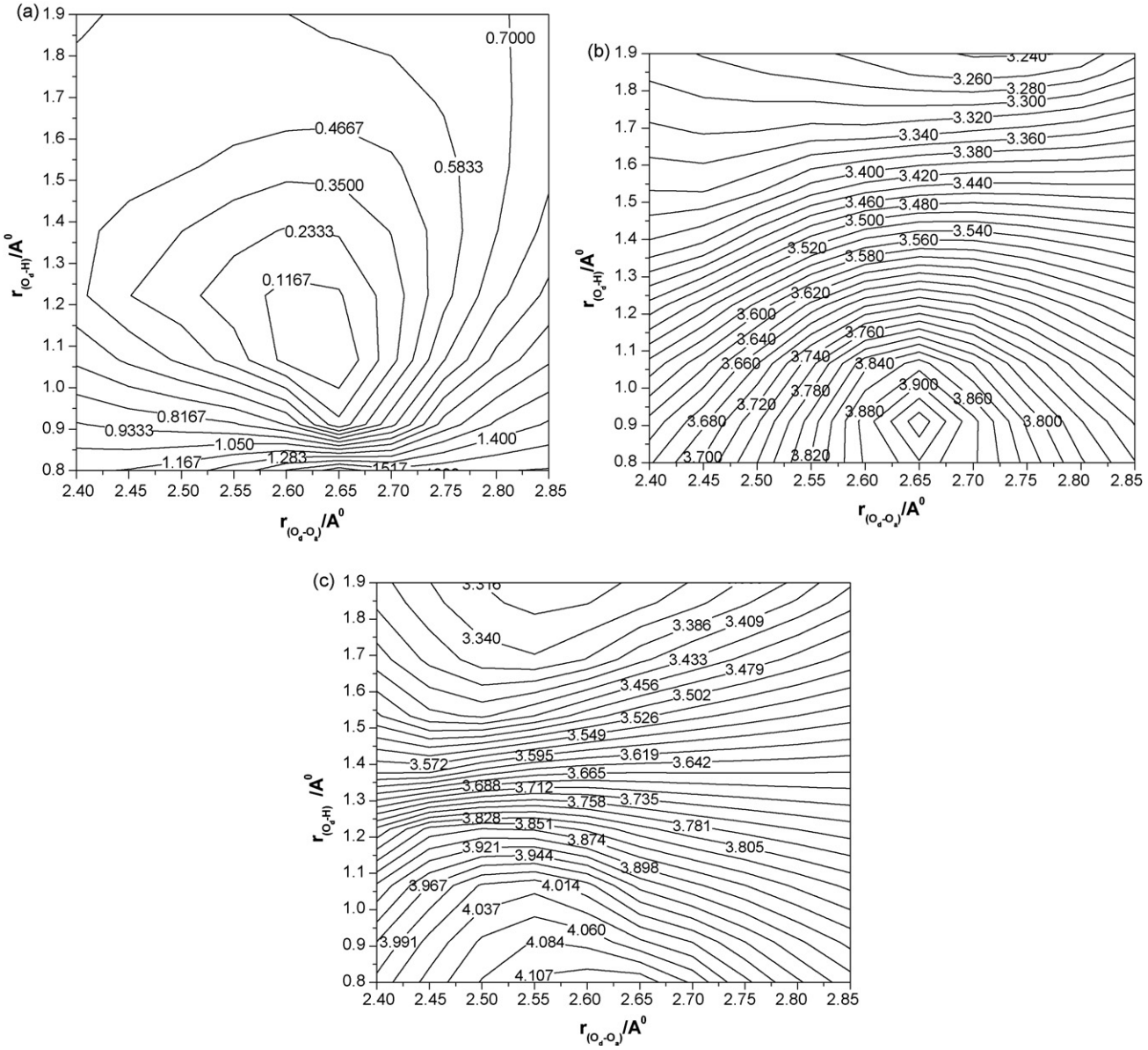

Fig. 5. 2D PESs for the (a) ground (S_0) state, (b) first excited singlet (S_1) state and (c) second excited singlet (S_2) state, plotted as a function of O_d–H and $O_d(2')$–$O_a(6')$ distances. The contour levels are the relative energies of the respective states in eV.

emission comes from the S_2 state of enol tautomer and emission of keto tautomer arises from its S_1 state. Catalan et al. [51] also reported structured, intensed absorption, fluorescence and excitation spectra involving S_0 and $S_2{}^{(\pi)}$ states.

Nagaoka et al. [50] observed that lifetime of the fluorescence emission of 'N' tautomer in the gas phase is about 0.5 ns [50] and that of keto tautomer in methyl cyclohexane is ~0.073 ns. [45]. Our calculated PES shows that energy gap between the ground and excited states for enol tautomer is much higher than the keto tautomer. Again according to the energy gap law, the higher the energy gap the higher is the lifetime. Thus our calculated PES supports nicely the relative trend of lifetime of the excited enol and keto tautomer.

Calculated potential energy profile (inset of Fig. 4) for S_0, S_1, and T_1 shows that $(S_0 < S_0') < (T_1' < T_1) < (S_1' < S_1)$ and this ordering of states are similar to case-C (potential energy surface) as reported by Kasha et al. [62]. They anticipate that the molecules having PES of the above type are the most typical of the proton transfer spectroscopy and this type of molecules can show both

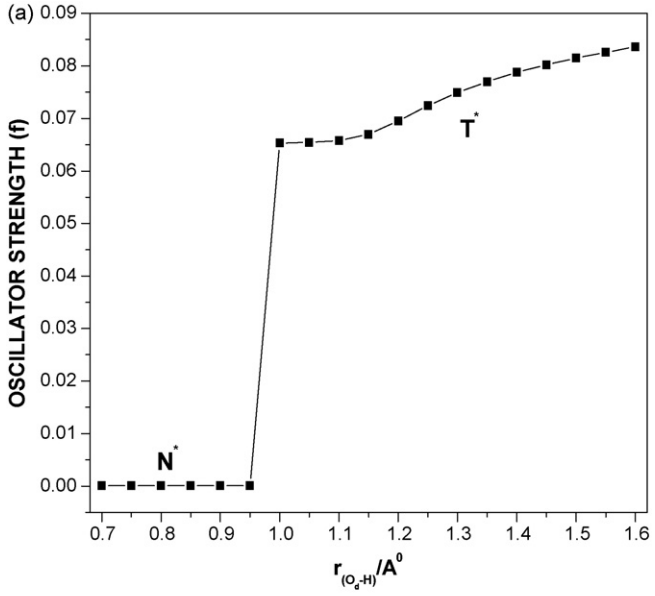

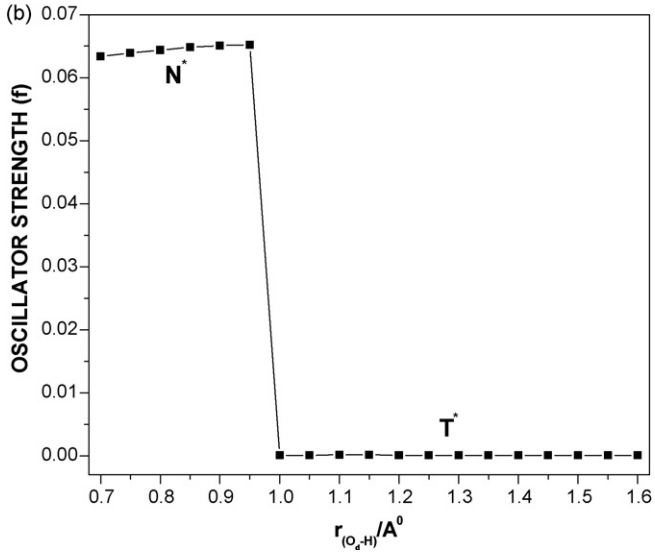

Fig. 6. Variation of the oscillator strengths with O_d–H distance in the (a) S_1 state and (b) S_2 state, computed using TD-DFT(B3LYP)/6-31G(d) level of theory.

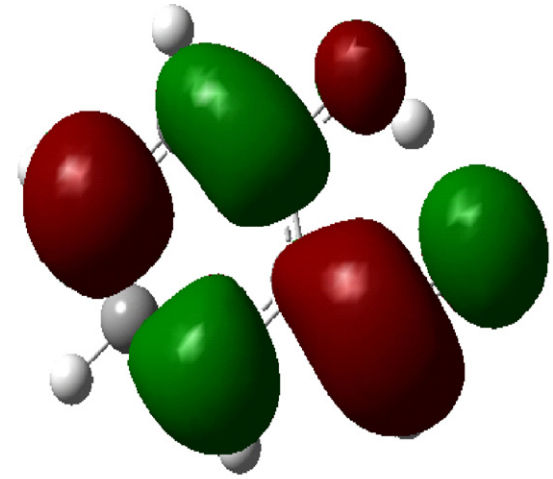

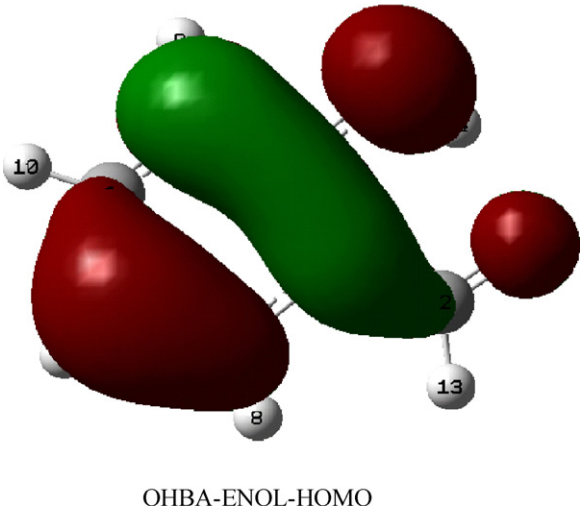

Fig. 7. HOMO and LUMO orbitals of OHBA (enol form) as obtained with DFT-B3LYP(6-31G(d)).

fluorescence ($S_1' \rightarrow S_0'$) and phosphorescence ($T_1' \rightarrow S_0'$) from its keto tautomer. Again a greater restriction on the observability of $T_1' \rightarrow S_0'$ emission will be the strong tendency to undergo radiationless intersystem crossing instead of appearing as a radiative process, as the $T_1' \rightarrow S_0'$ band gap decreases and the density of S_0' vibronic state at the T_1' zero point level increases.

Fig. 5a–c shows the PES with simultaneous variation of O_d–H and $O_d(2')$–$O_a(6')$ distances in the ground (S_0) state, first excited singlet (S_1) state and second excited singlet (S_2) state, respectively. The contour levels are given in relative energies and expressed in eV unit. In the S_0 state (Fig. 5a), the presence of a single valley corresponding to the enol ('N') form indicates that in the ground state enol form is the most stable structure. Whereas in the S_1 (Fig. 5b) and S_2 (Fig. 5c) states two valleys are observed corresponding to the excited enol (N*) and excited keto (T*) tautomers. Fig. 5b and c also illustrates a narrow potential well for N* and a much wider and deeper well for T* and thus indicating greater possibility of its existence over the N* form in the S_1 excited state. Although the S_2 state contains a high energy barrier between the N* and T* form, the contour diagram indicates the presence of both enol and keto forms in this state. It is due to the fact that the T* form present in the S_1 and S_2 states are isoenergetic in nature.

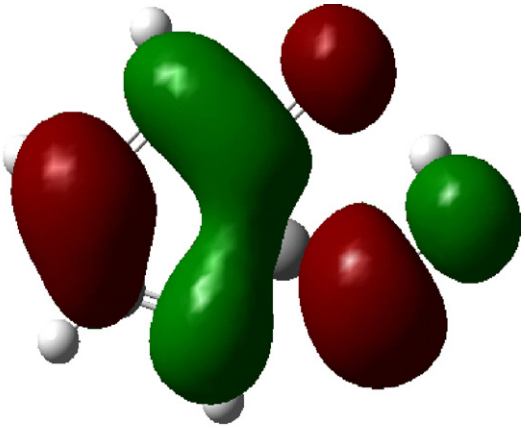

OHBA-KETO-LUMO

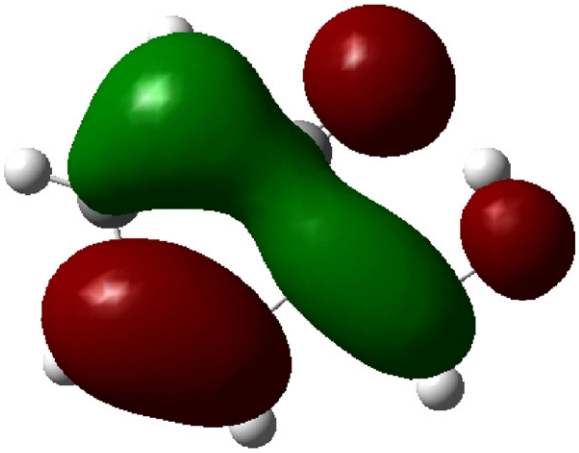

OHBA-KETO-HOMO

Fig. 8. HOMO and LUMO orbitals of OHBA (keto form) as obtained with DFT-B3LYP(6-31G(d)).

Variation of the oscillator strength with $r_{O_d(2')-H(1')}$ distance on going from N* to the T* form in the S_1 state are shown in fog.6a. It is observed that the calculated oscillator strength increases from N* to the T* in the S_1 state. This indicates high fluorescence quantum yield of T* form. Fig. 6b shows the variation of the same parameters in the S_2 state. The nature of this plot shows that oscillator strength decreases from N* form to the T* form. It supports the normal emission from this state. Thus the variation of oscillator strength with $r_{O_d(2')-H(1')}$ distance in the excited states supports the dual emission from two different states of OHBA.

An analysis of the electron density of HOMO and LUMO of OHBA can give us some idea about the ground and excited state proton transfer processes. Both HOMO and LUMO are of π type, but their phases are quite different in the enol and keto forms. HOMO orbital on the IMHB ring of OHBA (Fig. 7) is primarily of bonding character over the C(3′)C(4′)C(5′) atoms, where as C(3′)O(2′) and C(5′)O(6′) show anti-bonding character. Both the hydroxyl oxygen and carbonyl oxygen have bonding character, with a larger electron density over the hydroxyl oxygen. Analysis of HOMO π-electron density (Figs. 7 and 8) shows that the electron density on the hydroxyl oxygen (O(2′)) is relatively high compare to that on the carbonyl oxygen (O(6′)) of the 'N' tautomer. Again, after the transfer of proton along the proton transfer co-ordinate it is observed that the same oxygen atom, i.e. (O(2′)) still has higher electron density than (O(6′)) in the 'T' form. This observation supports the non-viability of ground state proton transfer.

On the other hand the LUMO is π^* in nature. If we look into the electronic charge distribution of LUMO within IMHB ring (N-tautomer), the C(4′)C(5′) position have bonding character, whereas C(3′)O(2′), C(3′)C(4′) and C(5′)O(6′) have antibonding character. Again, the LUMO of OHBA possess high electron density at O(6′) and comparatively low electron density at O(2′) than that of the corresponding HOMO. After tautomerization, LUMO of the keto-tautomer of OHBA shows comparable electron density on the O(6′) and O(2′) atom. In case of keto-tautomer of OHBA, both O(2′) and O(6′) atoms has comparable electron density. This observation suggests that the ESIPT process is favorable in OHBA.

4. Conclusions

In the OHBA molecule the strength of the IMHB is low enough. But this value is not sufficiently low to exhibit intramolecular proton transfer in the ground state. Free energy calculation, HOMO electron density and also ground state potential energy calculation for OHBA support the non-viability of GSIPT processes. On the other hand, excited state potential energy and LUMO electron density support the ESIPT process in OHBA. Moreover the PES shows that the enolic forms of OHBA in the first excited (S_1) and second excited singlet (S_2) state are almost isoenergetic. Again due to the high energy barrier in the S_2 state, the excited enol form (N*) cannot pass over to the excited keto form (T*). Thus the normal emission is observed from $S_2 \rightarrow S_0$ with comparatively greater intensity than that of $S_1 \rightarrow S_0$ emission. S_2 curve avoids the S_1 curve in the near vicinity of keto tautomeric form and the energy gap between these avoided curves is too small to observe any distinct emissive signature from these two states. PESs in terms of contour levels and the nature of variation of oscillator strength in the excited states nicely support this dual emission. Again, due to the very low energy gap between the first excited keto (T*) and excited enol (N*) tautomer of OHBA and the repulsive nature of the GSIPT curve and also due to the comparatively lower energy gap between S_0 and S_1 states in the keto positions of the compound, a red-shifted, broad and structureless emission band of OHBA is observed. Finally, Since all the calculations have been carried out by DFT method with hybrid functionals (B3LYP/6-31G(d)), it again supports the potentiality of DFT method for the calculations of ESIPT processes.

Acknowledgements

We gratefully acknowledge the financial support received from DST (Ref. No. SR/FTP/PS-60/2003) and UGC, New Delhi for carrying out this research work.

References

[1] P.T. Chou, D. MxMorrow, T.J. Aartsma, M. Kasha, J. Phys. Chem. 88 (1984) 4596.
[2] J. Catalan, J.L. Paz, J.C.D. Valle, M. Kasha, J. Phys. Chem. A 198 (1997) 5284.
[3] J. Keck, M. Roessler, C. Schroeder, G.J. Stueber, F. Waiblinger, M. Stein, D. Legourrierec, H.E.A. Kramer, H. Hoier, S. Henkel, P. Fischer, H. Port, T. Hirsch, G. Tytz, P. Hayoz, J. Phys. Chem. A 102 (1998) 6975.
[4] M.L. Martinej, W.C. Cooper, T.T. Chou, Chem. Phys. Lett. 193 (1992) 151.
[5] R.W. Munn, Chem. Br. (1989) 517.
[6] A. Sytnik, M. Kasha, Proc. Natl. Acad. Sci. U.S.A. 80 (1980) 8627.
[7] J. Catalan, J.C. Valle, J. Palomar, C. Diaz, J.L.G. Paz, J. Phys. Chem. A 103 (1999) 10921.
[8] T. Nishiya, S. Yamauchi, N. Hirota, Y. Fufiwara, M. Itah, J. Am. Chem. Soc. 108 (1986) 3880.
[9] C. Lu, R.M. Hsieh, L.R. Lee, P.Y. Cheng, Chem. Phys. Lett. 310 (1999) 103.
[10] J.A. Organero, M. Moreno, L. Santos, J.M. Lluch, A. Douhal, Chem. Phys. Lett. 328 (2000) 83.
[11] J.A. Organero, M. Moreno, L. Santos, J.M. Lluch, A. Douhal, J. Phys. Chem. A 104 (2000) 8424.

[12] S. Maheshwari, A. Chowdhury, N. Sathyamurthy, H. Mishra, H.B. Tripathi, M. Panda, J. Chandrasekhar, J. Phys. Chem. A 103 (1999) 6257.
[13] J. Catalan, J. Palomar, J.L.G. Paz, J. Phys. Chem. A 101 (1997) 7914.
[14] S. Nagaoka, Y. Shinde, K. Mukal, U. Nagashima, J. Phys. Chem. A 101 (1997) 3061.
[15] E. Orton, M.A. Morgan, G.C. Pimentel, J. Phys. Chem. 94 (1990) 7936.
[16] P.T. Chou, M.L. Martinez, S.L. Studer, J. Phys. Chem. 95 (1991) 10306.
[17] V. Vargas, L. Amigo, J. Chem. Soc., Perkin Trans. II (2001) 1124.
[18] L. Antonov, W.M.F. Fabian, D. Nedltcheva, F.S. Kamounah, J. Chem. Soc., Perkin Trans. II (2000) 1173.
[19] S.H. Alarcon, A.C. Olivieri, D. Sanz, R.M. Claramunt, J. Elguero, J. Mol. Struct. 705 (2004) 1.
[20] I.K. Starzomska, A. Filarowski, M. Rospenk, A. Koll, S. Mlikova, J. Phys. Chem. 108A (2004) 2131.
[21] A. Weller, Z. Elektrochem. 60 (1956) 1144.
[22] A. Weller, Prog. React. Kinet. 1 (1961) 187.
[23] F. Lahmani, A. Zehnacker-Rentien, J. Phys. Chem. A 101 (1997) 6141.
[24] D. Gormin, A. Sytnik, M. Kasha, J. Phys. Chem. A 101 (1997) 672.
[25] P.F. McGarry, S. Jockusch, Y. Fujiwara, N.A. Kaprinidis, N.J. Turro, J. Phys. Chem. A 101 (1977) 764.
[26] V. Guallar, M. Moreno, J.M. Lluch, F. Amat-Guerri, A. Douhal, J. Phys. Chem. 100 (1996) 19789.
[27] J. Keck, H.E.A. Kramer, H. Port, T. Hirsch, P. Fischer, G. Rytz, J. Phys. Chem. 100 (1996) 14468.
[28] F. Parsapour, D.F. Kelley, J. Phys. Chem. 100 (1996) 2791.
[29] R.M. Tarkka, S.A. Jenekhe, Chem. Phys. Lett. 260 (1996) 533.
[30] H. Zhang, P. van der Meulen, M. Glasbeek, Chem. Phys. Lett. 253 (1996) 97.
[31] S. Mitra, R. Das, S.P. Bhattacharyya, S. Mukherjee, J. Phys. Chem. A 101 (1997) 293.
[32] P.G. Yi, Y.H. Liang, C.Z. Cao, Chem. Phys. 315 (2005) 297.
[33] S. Nagaoka, U. Nagashima, J. Phys. Chem. 94 (1990) 1425.
[34] S. Nagaoka, U. Nagashima, Chem. Phys. 136 (1989) 153.
[35] M.V. Verner, S. Scheiner, J. Phys. Chem. 99 (1995) 642.
[36] A.L. Sobolewski, W. Domcke, Chem. Phys. 184 (1994) 115.
[37] J. Catalan, J. Palomar, J.L.G. De Paz, J. Phys. Chem. A 101 (1997) 7914.
[38] K.-Y. Law, J. Shoham, J. Phys. Chem. 98 (1994) 3114.
[39] K.-Y. Law, J. Shoham, J. Phys. Chem. 99 (1995) 12103.
[40] A.U. Acuna, F. Toribio, F. Amat-Guerri, J. Catalan, J. Photochem. 30 (1985) 339.
[41] F. Toribio, J. Catalan, F. Amat, A.U. Acuna, J. Phys. Chem. 87 (1983) 817.
[42] A.U. Acuna, F. Amat-Guerri, J. Catalan, F. Gonzalez-Tablas, J. Phys. Chem. 84 (1980) 629.
[43] J. Goodman, L.E. Brus, J. Am. Chem. Soc. 100 (1978) 7472.
[44] K.K. Smith, K.J. Kaufmann, J. Phys. Chem. 82 (1978) 2286.
[45] S. Nagaoka, N. Hirota, M. Sumitani, K. Yoshihara, J. Am. Chem. Soc. 105 (1983) 4220.
[46] T. Nishiya, S. Yamauchi, N. Hirota, M. Baba, I. Hanazaki, J. Phys. Chem. 90 (1986) 5730.
[47] L.A. Peteanu, R.A. Mathies, J. Phys. Chem. 96 (1992) 6910.
[48] M.A. Morgan, E. Orton, G.C. Pimentel, J. Phys. Chem. 94 (1990) 7927.
[49] S. Nagaoka, N. Hirota, M. Sumitani, K. Yoshihara, E. Lipezynska-Kochany, H. Iwamura, J. Am. Chem. Soc. 106 (1984) 6913.
[50] S. Nagaoka, U. Nagashima, N. Ohta, M. Fujita, T. Takemura, J. Phys. Chem. 92 (1988) 166.
[51] J. Catalan, F. Toribio, A.U. Acuna, J. Phys. Chem. 86 (1982) 303.
[52] A. Dreuw, M.H. Gordon, Chem. Rev. 105 (2005) 4009.
[53] J. Catalan, J.C. delvalle, J. Palomer, C. Diaz, J.L.G. dePaz, J. Phys. Chem. A 103 (1999) 10921.
[54] A.D. Becke, J. Chem. Phys. 98 (1993) 5648;
C. Lee, W. Yang, R.G. Parr, Phys. Rev. B 37 (1988) 785.
[55] V. Barone, C. Adamo, J. Phys. Chem. 99 (1995) 15062.
[56] A. Datta, S.S. Mallajosyula, S.K. Pati, Acc. Chem. Res. 40 (2007) 213.
[57] M.J. Frisch, G.W. Trucks, H.B. Schlegel, G.E. Scuseria, M.A. Robb, J.R. Cheeseman, J.A. Montgomery Jr., T. Vreven, K.N. Kudin, J.C. Burant, J.M. Millam, S.S. Iyengar, J. Tomasi, V. Barone, B. Mennucci, M. Cossi, G. Scalmani, N. Rega, G.A. Petersson, H. Nakatsuji, M. Hada, M. Ehara, K. Toyota, R. Fukuda, J. Hasegawa, M. Ishida, T. Nakajima, Y. Honda, O. Kitao, H. Nakai, M. Klene, X. Li, J.E. Knox, H.P. Hratchian, J.B. Cross, C. Adamo, J. Jaramillo, R. Gomperts, R.E. Stratmann, O. Yazyev, A.J. Austin, R. Cammi, C. Pomelli, J.W. Ochterski, P.Y. Ayala, K. Morokuma, G. A. Voth, P. Salvador, J.J. Dannenberg, V.G. Zakrzewski, S. Dapprich, A.D. Daniels, M.C. Strain, O. Farkas, D.K. Malick, A.D. Rabuck, K. Raghavachari, J.B. Foresman, J.V. Ortiz, Q. Cui, A.G. Baboul, S. Clifford, J. Cioslowski, B. B. Stefanov, G. Liu, A. Liashenko, P. Piskorz, I. Komaromi, R.L. Martin, D.J. Fox, T. Keith, M.A. Al-Laham, C.Y. Peng, A. Nanayakkara, M. Challacombe, P.M.W. Gill, B. Johnson, W. Chen, M. W. Wong, C. Gonzalez, J. A. Pople, Gaussian 03, Revision C.02, Gaussian, Inc., Wallingford CT, 2004.
[58] S.P. De, S. Ash, S. Dalai, A. Misra, J. Mol. Struct. (THEOCHEM) 807 (2007) 33.
[59] S.P. De, S. Ash, H. Bar, D.K. Bhui, S. Dalai, A. Misra, J. Mol. Struct. (THEOCHEM) 824 (2007) 8.
[60] A.L. Sobolewski, W. Domcke, Chem. Phys. 232 (1998) 257.
[61] I.M. Hunsberger, J. Am. Chem. Soc. 72 (1950) 5626.
[62] M. Kasha, J. Heldt, D. Gormin, J. Phys. Chem. 99 (1995) 7281.